Master in Nanostructured Materials
for Nanotechnological Applications

Ordered mesoporous silica monoliths: synthesis, preparation and potential applications

University of Zaragoza
Institute of Nanoscience of Aragón
Nanoporous Films and Particles Group

Author: María Gracia Colmenares Quevedo
Directors: Manuel Arruebo Gordo
Francisco Balas Nieto

Thanks to all the people who helped make this possible.

María Gracia

Contents

I. Introduction and Objectives

The work carried out is a part of the research line being conducted by the Nanoporous Films and Particles Group (NFP), of the Institute of Nanoscience of Aragon (INA) in the University of Zaragoza, regarding mesoporous materials synthesis and applications. This project comprises the preparation and characterization of *rigid bimodal mesoporous silica monoliths*, in order to investigate their potential applications as controlled drug release matrices. All work was based on the hexagonally-ordered mesoporous SBA-15 materials. Drug release experiments include release of the antibiotic cefuroxime from as-synthesized and amino-functionalized SBA-15 powders and monoliths.

Previous work carried out by the NFP group in controlled drug release has proven that drug loading and release kinetics vary in modified and unmodified mesoporous silica SBA-15 powders, resulting in higher loadings and controlled release from functionalized materials (Carmona and Balas, unpublished data). Our monolithic structures have a bimodal pore structure, this is, the characteristic mesopores of SBA-15 and an array of interstitial macropores that may also function as drug reservoirs and affect diffusion of the drug. Moreover, the rigid monolithic structure has potential in functioning as an implantable drug delivery vehicle to be applied in traumatology and orthopedic surgery. One of the objectives of this work is to compare drug loading and release profiles of amino-modified and unmodified SBA-15 powders and the newly-prepared monoliths alike, in order to establish advantages and disadvantages and further investigate potential drug-delivery applications.

The overall aim of this project is to present the synthesis and characterization of rigid SBA-15 monoliths and to introduce the study of potential applications in controlled drug delivery. A theoretical background including key definitions and previous and current relative work is presented; the experimental protocols employed for preparation and testing of the materials under study are detailed, and final results are discussed.

II. Theoretical Background

In this chapter, an overview of mesoporous materials, with an emphasis on mesoporous silica, is presented. Synthesis methods are reviewed, as well as some background regarding potential applications of mesoporous silica monolithic structures in the field of drug delivery.

II.1. MESOPOROUS MATERIALS: MESOPOROUS SILICAS

II.1.1. General considerations on porous solids

Most solid materials, natural or synthetic, are porous to some extent. A porous solid can be defined as that which contains cavities, channels or interstices which are deeper than they are wide. These cavities, or pores, can be classified according to their availability to an external fluid or their shape[1], as follows:

Table II.1. Pore classification.

	Type of pore	Description
Availability to an external fluid	Closed pores	Completely isolated pores (Fig. II.1, a)
	Open pores	Continuous channel of communication with external surface (Fig. II.1, b, c, d, e, f)
	Blind pores	Open on one end (Fig. II.1, b, f)
	Through pores	Open on two ends (Fig. II.1, e)
Shape	Cylindrical	Either open (Fig. II.1, c) or blind (Fig. II.1, f)
	Ink-bottle	(Fig. II.1, b)
	Funnel-shaped	(Fig. II.1, d)
	Slit-shaped	(Fig. II.1, c)

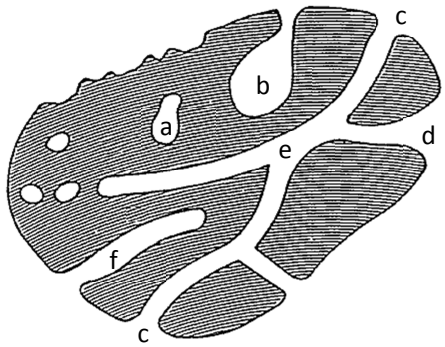

Fig. II.1. Schematic cross-section of a porous solid[1].

Some porous materials are defined as *consolidated*, which means that they exists as a relatively rigid macroscopic body whose dimensions exceed those of the pores by many orders of magnitude; they may be called *agglomerates*, or in the particular case in study, ***monoliths*** (from the Greek *mono*, single and *lithos*, stone). Others can be defined as *unconsolidated*, being non-rigid, loosely packed assemblages of individual particles; they may be called *aggregates*.

These materials can be formed naturally or synthetically by several different routes. Pores can be an inherent characteristic of crystalline materials, with the pore size general being limited to molecular dimensions within a highly regular network. On the other hand, pores can be a result of constitutive processes in which aggregation and subsequent agglomeration of loose particles results in materials whose final structure depends on the original arrangement of the primary particles and their size. A third route is described as ***subtractive***, in which certain elements of the original structure are selectively removed to create pores[1]. The latter is the route employed in the present study.

It is necessary to define basic terms that correspond to characteristics of porous solids that were studied in the present investigation. These include:

- Pore size: distance between opposite walls of the pore (for example, diameter of cylindrical pores). This property is of major importance in practical applications of porous materials, as pore size directly affects selectivity and dictates the diffusion process through the material.
- Pore volume: volume of pores as measured by any given method.
- Specific surface area: accessible or detectable area of solid per unit mass of material.
- Porosity: ratio of total pore volume to the apparent volume of the particle or powder (excluding interstitial voids, unless otherwise specified).

According to the IUPAC notation, mesoporous materials can be defined those with a pore diameter between 2 and 50 nm, between the pore sizes that define micro and macroporous materials. They have characteristic high surface areas, which make them particularly useful for a wide number of applications.

II.1.2. Mesoporous materials

Mesoporous materials synthesis was initially focused on silica-based materials. The first mesoporous materials synthesized were described in a patent from 1971 and resulted in the preparation of a low-density, surfactant-templated silica-based solid[2,3]. This invention, however, was practically ignored in the sense of a mesoporous material and it was not until the early 1990s when researchers in Japan[4] synthesized and characterized a novel mesoporous silica solid, resulting in the formation of three-dimensional SiO_2 networks with tunable pore sizes ranging from 2 to 4 nm. In the mid-1990s, Mobil Corporation Laboratories produced similar materials with a well-defined ordered pore structure, under the name Mobile Composition of Matter, or MCM[5], intended to be used as molecular sieves, given that pore size control was achieved resulting in potentially more selective materials.

In the past fifteen years, mesoporous materials research has focused mainly on synthesis and structures; methods of synthesis covered in the most cited papers from this time period include block copolymer templating[6] and triblock copolymer synthesis[7], among others. Structures of particular interest include mesoporous materials with hybrid organic/inorganic frameworks[8] and crystalline or semi-crystalline frameworks[9]. Applications of said mesoporous materials mainly cover the areas where molecular recognition is necessary or useful, controlled drug delivery[10], sensing[11], and molecular sieving[12], amongst others.

Preparation of non-oxide materials with mesoporous structures has played an especially important role in the 21st century, beginning with the invention of mesoporous carbon materials[13]. New families of mesoporous materials have been created due to these trends in research. Non-siliceous ordered mesoporous materials are by now accessible in a wide range of compositions[14].

Ordered mesoporous silicas, however, are still an important and ongoing field of research, and new biomedical applications focus mainly on drug release, including research on release via mesoporous silica coating of magnetic nanoparticles, smart (stimuli-responsive) drug delivery systems, etc. Other applications of mesoporous silica currently under study include templating to obtain metal nanowires, nanoreactor technology and as supports for noble metal nanoparticle catalysts.

II.1.3. Ordered mesoporous silica: SBA-15 synthesis

Well-known nanoporous siliceous materials are zeolites, which provide excellent catalytic properties by virtue of their crystalline nanostructured aluminosilicate network. However, their applications are limited by the relatively small pore openings (<1nm); therefore, pore enlargement was one of the main aspects in zeolite chemistry. Larger pores are present in porous glasses and porous gels which were known as mesoporous materials at the time of the discovery of MCM-41. However, they showed disordered pore systems with broad pore size distributions.

With MCM-41, the first mesoporous solid with a regularly ordered pore arrangement and a very narrow pore size distribution was achieved. The original MCM-41 synthesis was carried out in water under alkaline conditions. In the same way as zeolite synthesis, organic molecules (surfactants) function as templates forming an ordered organic–inorganic composite material. In the broadest sense a template may be defined as a central structure about which a network forms in such a way that removal of the template creates a cavity with morphological features related to those of the template[15]. Via calcination or extraction the surfactant is removed, leaving the porous siliceous network. However, in contrast to zeolites, the templates are not single organic molecules but liquid-crystalline self-assembled surfactant molecules (see Fig. II.2). The formation of the inorganic-organic composites is based on electrostatic interactions between the positively charged surfactants and the negatively charged siliceous species.

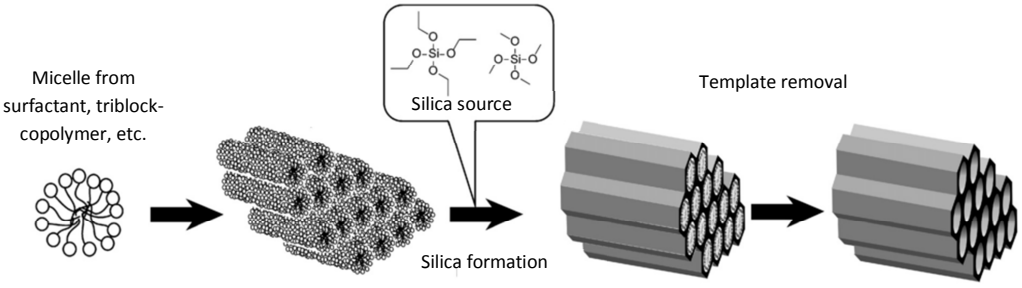

Fig. II.2. General concept for synthesis of mesoporous silica from micelle template[16].

The liquid-crystal-controlled synthesis of MCM-41 opened a wide variety of synthesis approaches for developing new materials. The successful preparation of new porous materials

could be achieved by developing new synthesis pathways and by taking advantage of the liquid-crystal chemistry provided by the surfactant.

The original approach was extended to the use of triblock copolymer templates under acidic conditions, by which means the Santa Barbara Amorphous (SBA) silica phases were synthesized[7]. The material under study, SBA-15, is characterized by a large BET surface area (>700m2/g) with large pore diameter (~ 8nm) and large pore wall thickness. The large wall thickness results in higher hydrothermal stability than M41S materials[17]. Furthermore, SBA-15 exhibits continuous porous channels and has a characteristic hexagonal structure (*p6mm*)[18].

In the case of SBA-15 synthesis, a nonionic triblock copolymer, namely Pluronic (P123)[19] is used as a micelle template. P123 is one of the Pluronics triblock copolymers, which are composed of a central hydrophobic chain of polyoxypropylene flanked by two hydrophilic chains of polyoxyethylene (see Fig. II.3); its nominal chemical formula is $HO(CH_2CH_2O)_{20}(CH_2CH(CH_3)O)_{70}(CH_2CH_2O)_{20}H$, which corresponds to a molecular weight of about 5800 Da.

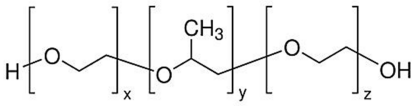

Fig. II.3. Molecular structure of Pluronics® triblock copolymers.

Because of their amphiphilic structure, these triblock copolymers have surfactant properties that make them useful in many applications. As a result of their amphiphilic nature, surfactants can associate into supramolecular arrays, forming micelles with a configuration that depends on the nature of the solvent (an aqueous solvent, for example, would lead to micelles with hydrophobic centers and hydrophilic tails). The extent of micellization, the shape of the micelles, and the aggregation of micelles into liquid crystals depend on the surfactant concentration. At slightly higher concentrations, called the critical micelle concentration (CMC1), the individual surfactant molecules form small, spherical aggregates (micelles). At higher concentrations (CMC2), where the amount of solvent available between the micelles decreases, spherical micelles can coalesce to form elongated cylindrical micelles (characteristic templates for SBA-15). At slightly higher concentrations, liquid-crystalline (LC) phases form; as concentration increases, rodlike micelles aggregate to form hexagonal close-packed LC arrays and cubic bicontinuous LC phases form followed by LC lamellar phases[20].

The silica source employed for SBA-15 synthesis is the metal alkoxide tetraethyl orthosilicate (TEOS), which is a tetrahedral molecule consisting of four ethyl groups attached to a SiO_4^{4-} ion, called an *orthosilicate* (see Fig. II.4). The nominal chemical formula of TEOS is $Si(OC_2H_5)_4$.

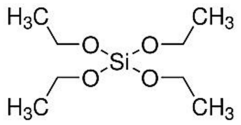

Fig. II.4. Molecular structure of tetraethylorthosilicate (TEOS).

The synthesis of mesoporous silica follows a metal alkoxide-based sol-gel reaction. The sol-gel transition of a metal alkoxide solution is generally caused by two kinds of reactions, i.e.,

hydrolysis and polycondensation. Although the former one is necessary for the latter to take place, these reactions are known to proceed in parallel from a very early stage of the whole reaction[21]. In usual cases, the hydrolysis is initiated by mixing water with alkoxide in the presence of alcohol as a co-solvent (Ec. II.1). The hydrolysis of M-OR produces M-OH which subsequently condenses with other M-OH to produce a polycondensed species containing an M-O-M linkage and water (Ec. II.2). A successive condensation leads to the growth of metaloxane oligomers which subsequently link together to form a gel network (Ec. II.3). In the presence of a limited amount of water, the alcohol producing condensation is also possible. The overall reactions for silicon alkoxide, $Si(OR)_4$ are expressed as follows:

$$Si(OR)_4 + H_2O \rightarrow Si(OH)(OR)_3 + ROH \quad \text{...(Ec. II.1)}$$

$$Si - OH + Si - OH \rightarrow Si - O - Si + H_2O \quad \text{...(Ec. II.2)}$$

$$Si - OH + Si - OR \rightarrow Si - O - Si + ROH \quad \text{...(Ec. II.3)}$$

TEOS has the remarkable property of easily converting into silicon dioxide; a silica network with silanol groups on the external surface is obtained and the side product is ethanol. Silicon alkoxides exhibit extraordinarily slow hydrolysis and polycondensation kinetics compared to other metal alkoxides. For this reason, a controlled hydrolysis of silicon alkoxides is much easier and the silica gel materials can be processed into various morphologies by varying the processing method. The reaction proceeds as was described above, in summary:

$$Si(OC_2H_5)_4 + 2H_2O \rightarrow SiO_2 + 4C_2H_5O \quad \text{...(Ec. II.4)}$$

For the case of SBA-15 synthesis, TEOS molecules are condensed on the hydrophilic surface of cylindrical micelles, ensuring that a faithful replica of the template is obtained. A fundamental condition for these methods of synthesis is that an attractive interaction between the template and the silica precursor is produced to ensure inclusion of the structure director without phase separation taking place. Interactions between nonionic templates (as P123) and silica sources are mediated through hydrogen bonds[22]. The structure of the wall of the resulting pores consists of a disordered net- work of siloxane bridges and free silanol groups ; this framework is well suited for the development of bonded selective sorption phases, via functionalization with organic molecules (see section III.1).

II.2. BIMODAL MESOPOROUS SILICA MONOLITHS

Mesoporous silicas were initially synthesized exclusively as powders, which made them suitable for catalytic and separation applications, with a variety of ordered mesophase architectures available (cubic, hexagonal, lamellar, etc), as was mentioned previously. Since then, however, efforts to improve the processability and broaden application possibilities of these materials have been made, resulting in low-molecular weight surfactant/inorganic mesophase composites and mesoporous solids in the form of films, spheres, etc.

Optically transparent silica/block copolymer monoliths have been synthesized with high degrees of mesoscopic order, by means of solvent evaporation within the mesostructure (note that the natural meaning of monolith is a geological feature such as a mountain, consisting of a

single massive stone or rock)[23,24]. These monoliths, although rigid and free of cracks, are not mesoporous materials, but mesostructured composites as the block copolymer template is not removed after synthesis[25].

Monolithic silicas with well-defined porous structures have been mainly focused on investigations for applications in separations. HPLC columns based on such materials were first reported in 1996[26], and are characterized by higher total porosity and permeability compared to packed columns, allowing operation at low pressures, yet at higher flow rates, thus reducing the analysis time drastically. Monolithic silica HPLC columns are already marketed by Merck Co. under the trade name Chromolith™. These monoliths are readily prepared inside HPLC columns, for exclusive use in chromatography.

For many applications, such as size selective adsorption[27] materials with both small and large pores arranged in a hierarchical structure-in-structure fashion are desirable. So-called bimodal silica monoliths were first synthesized by Nakanishi, et. al. in 2005 by direct synthesis[28], resulting in confined monoliths with an ordered hierarchical porous structure.

A common problem regarding preparation said structures, however, is that they tend to be mechanically unstable unless encapsulated or embedded in a polymeric network (i.e., monoliths tend to crack upon calcination and removing from the mold, yielding irregular pieces and coarse powders, especially as the diameter of the monolith decreases). Leventis, et. al., prepared polymer-encapsulated bimodal monoliths with increased mechanic stability. The same study includes attempts to prepare monoliths without polymeric encapsulation, proving unsuccessful[29].

In response to this and due to the important amount of potential applications, various techniques for synthesizing silica monoliths with an ordered macro/mesoporous structure were developed. Bimodal macro/mesoporous silica monoliths can be prepared in two ways: by direct-templating of mesoporous silica in a mold that holds the desired shape of the monolith (dual-templating techniques[30]), and by using as-synthesized or modified mesoporous silica within a polymeric network that aids in holding the desired shape[31]. Another preparation method is by controlled fusion of mesoporous spherical silica particles[32], yielding mechanically stable monoliths with tunable open macropores and surfactant-templated ordered mesopores.

Recent advances in research concerning hierarchically ordered mesoporous silica monoliths are focused mainly on applications in catalysis and as catalytic reactors. These monolith rods were used as continuous flow catalytic microreactors after introduction of the active sites via grafting of organic functions, or via the transformation of the amorphous silica skeleton into other mesoporous silica species. These monolithic reactors demonstrated higher productivities than batch or packed-bed reactors for various model reactions[33].

II.3. CONTROLLED DRUG DELIVERY

In the present study, silica monoliths exhibiting macropores of approximately 3 μm and mesopores ranging from 5 to 7 nm were prepared for testing in controlled drug delivery of an antibiotic as a model drug.

Drug delivery is a key factor contributing to the therapeutic and commercial potential of many drugs and related products. It is the driving force behind the development of many new devices and formulation-based projects.

Conventional forms of drug delivery include oral, topical, inhaled, injections, etc. However, more sophisticated delivery systems must take into account pharmacokinetic principles, specific drug characteristics and variability of response - from one person to another and within the same person under different conditions. The therapeutic efficiency of a drug can be enhanced and toxic effects reduced if, for example, the amount and persistence of the drug in the vicinity of the target cells is increased, while reducing exposure of the drug to non-targeted cells.

Design of any drug delivery system (DDS) must simultaneously take into consideration factors such as[34]:

- drug properties
- biocompatibility
- targeting abilities
- nature of delivery vehicle
- mechanism of drug release
- duration of delivery
- route of administration

These are the principles behind *controlled drug delivery*. It is not easy, however, to achieve all these factors in one system because of their extensive independency. Various approaches for controlled drug delivery are briefly described below[34]:

a) **Localized drug delivery:** It is desired in many cases to deliver drugs at a specific site inside the body, to a particular diseased tissue or organ, especially for drugs that tend to provoke unintended side effects that can be severe (i.e. anticancer drugs, anti-inflammatory steroids, etc.).
b) **Targeted drug delivery:** Delivery would typically involve a recognition event between the drug carrier and specific receptors at the cell or tissue surface. The concept of targeted drug delivery differs from localized delivery in the sense that the latter simply implies localization of the delivery vehicle in the vicinity of an organ or tissue site, while targeting is based on delivery to specific cell or tissue types.
c) **Sustained drug delivery (Zero order release profile):** Ideally, the blood level of a drug would remain constant throughout the delivery period, yielding a continuous release profile consistent with zero-order kinetics[35]. However, injected or ingested drugs follow first-order kinetics, with high blood levels after initial administration (which could result in toxicity) followed by a rapid decrease in blood concentration (resulting in low drug efficacy). This drug release profile is undesirable; advantages of a continuous release include reduced risk of toxic effects, predictable and extended duration of drug action, and reduced frequency of dosing. See Fig. II.5.

d) **Modulated drug delivery (nonzero-order release profile):** Patterning release profile still remains a great challenge in drug delivery. A delivery system with a manipulable nonzero-order profile would ideally be tunable to each situation.
e) **Feedback controlled drug delivery:** The ideal drug delivery system is the feedback controlled system, consisting of drug release in response to a therapeutic marker. Two classes can be defined: modulated devices, in which monitoring the chemical environment is possible in order to change the delivery rate continuously, and triggered devices, in which no release takes place until it is triggered by a marker or an external stimuli.
f) **Implantable controlled drug delivery devices:** implantable devices are very attractive for a number of classes of drugs, particularly those that cannot be delivered via the oral route or are irregularly absorbed via the gastrointestinal tract. For certain diseases that require chronic administration of drugs, an implantable release device is highly useful. The monoliths developed in this project have a potential use as implantable controlled drug delivery devices applied in traumatology and orthopedic surgery. In these scenarios, bacterial infection after implantation is very common, making antibiotic-delivering implants an attractive option. Moreover, in cases where bone regeneration is necessary, the controlled release of growth factors may enhance the healing process after a fracture.

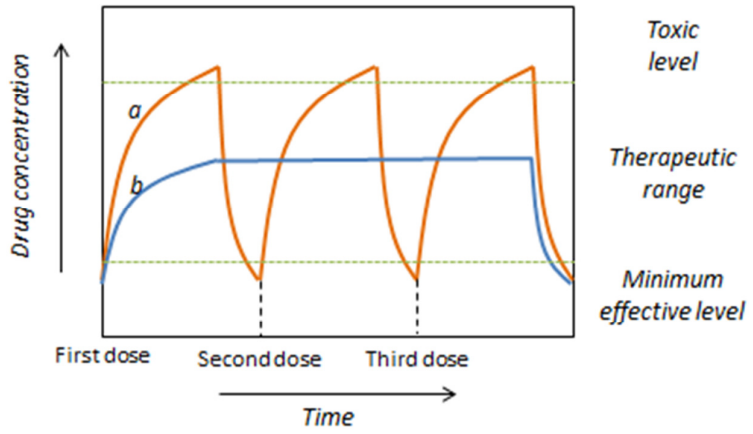

Fig. II.5. Zero-order (b) and first-order (a) kinetic profiles. A zero-order profile is preferable, as only one dose is necessary to maintain constant drug concentration within the therapeutic range for a prolonged period of time.

Important parameters to consider in the design of a drug delivery vehicle include[36]:

a) use of biocompatible materials with simple robust processes for biomaterial assembly, conjugation chemistry, and purification steps;
b) ability to optimize in parallel the numerous biophysicochemical parameters of targeted drug delivery vehicles important for pharmacokinetic control and possible cell uptake; and
c) development of scalable unit operations amenable to manufacturing large quantities of targeted drug delivery systems needed for clinical translation.

One of the applications of the present investigation is based on the study of the release of a model antibiotic (namely cefuroxime sodium salt) from mesoporous powder and bimodal monolithic SBA-15, in order to assess differences between morphologies and pure-silica functionalized surfaces. Cefuroxime is a type of antibiotic called a cephalosporin, related to penicillin. First-generation cephalosporins are active predominantly against Gram-positive bacteria, and successive generations have increased activity against Gram-negative bacteria.

The impact of mesoporous silica as a drug delivery vehicle is described below.

Mesoporous silica in drug delivery

Mesoporous silica matrices have been investigated as potential drug carriers due to the following features[37]:

a) Ordered pore network: as was previously described, mesoporous silica has a characteristic highly ordered array of pores whose structure depends on synthesis conditions. The ordered mesopore network is therefore tunable very homogeneous in size, allowing fine control of drug loading and release kinetics;
b) High pore volume: large drug loads are viable;
c) High surface area: implies high potential for drug adsorption;
d) Silanol-covered surface: possible functionalization to allow better control over drug loading and release;
e) Biocompatibility[38].

Various studies of release of model drug molecules from mesoporous silica matrices of different pore sizes have been carried out, suggesting that several factors could affect the release profile of the hosted molecule. Studies on release of model drug molecules of different molecular sizes from mesoporous silicas with a cubic pore ordering[39] indicated that release tends to become slower as the pore size of the matrix decreases or the molecular size of the drug increases, and release rate was decreased further by functionalizing the mesopore wall (see following section). Comparison studies of release of a model antibiotic from hexagonally-ordered mesoporous silica powder and discs[40], resulting in release with a higher degree of control than conventional presentations of the antibiotic. It was also observed that release was slower and more controlled from disks than from powders.

Organic-modified mesoporous silica

The interaction between mesoporous matrices and drugs is also decisive for designing controlled drug delivery systems for clinical applications; the drug-material interaction is determinant regarding the adsorption and delivery behavior of the drug. One of the characteristics of mesoporous silica materials is the presence of a high concentration of silanol groups in the mesopores, which can be functionalized for the control of pore size and surface properties. Reactive and passive organic groups can be incorporated into the solid either by simultaneous condensation of corresponding silica and organosilica precursors (co-condensation), by incorporating organic groups as bridging components directly and specifically into the pore walls by the use of bis-silylated single-source organosilica precursors

(production of periodic mesoporous organosilicas) or by subsequent modification of the pore surface of a purely inorganic silica material (grafting)[22].

In the present study, SBA-15 was modified by grafting, which refers to the subsequent modification of the inner surfaces of mesostructured silica phases with organic groups. This process is carried out primarily by reaction of organosilanes of the type $(R'O)_3SiR$; in principle, it's possible to functionalize with a variety of organic groups by modifying the organic residue (see Fig. II.6).

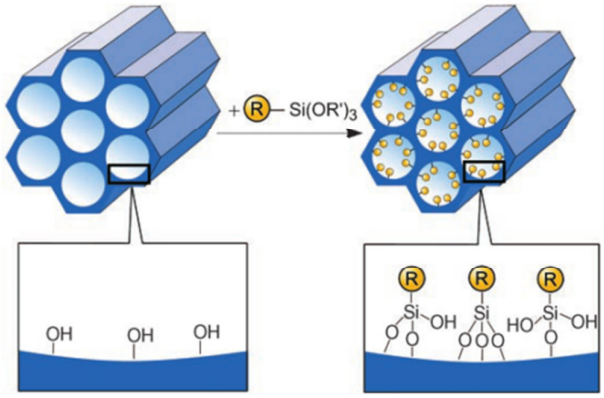

Fig. II.6. Grafting for organic modification of mesoporous silica with terminal organosilanes[22].

It must be taken into account that functionalization involves a decrease in pore size, which can directly affect the release kinetics, especially for drugs with a size similar to that of the pore diameter[41].

Several investigations of drug release from functionalized mesoporous silica have been reported. Functionalization of SBA-15 with long alkyl chains resulted in a decreased release rate compared to as-calcined SBA-15[41]. Postsynthesis amine-functionalized SBA-15 yielded more control of release kinetics than the as-calcined samples: ibuprofen release rates were improved due to presence of ionic interaction between carboxyl groups in ibuprofen and amine groups on the surface of SBA-15, and release of bovine serum albumin (BSA) was improved due to o the balance of electrostatic interaction and hydrophilic interaction between BSA and the SBA-15 matrix[10].

Drug release profiles and kinetics

The drug delivery profile is very relevant in the design of a drug delivery system. Release kinetics can be optimized by understanding the release process and determining the release mechanism. For many DDS, the drug release process can be modeled by a dissolution profile. For mesoporous silica, it has been shown that drug release is diffusion controlled[40,42], making it possible to calculate kinetic parameters for comparison purposes.

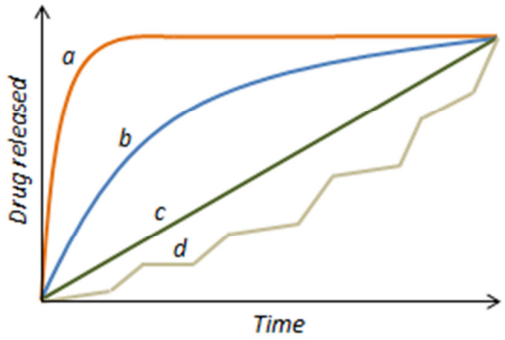

Fig. II.7. Common release profiles for mesoporous materials[37].

Fig. II.7 shows common release profiles for mesoporous materials[37]. Profile *a* corresponds to unmodified surfaces, in which an initial burst release is followed by a slow release; this profile is desirable when an immediate high dose is required, as in acute infections. Profile *b* is associated with diffusion or dissolution processes, and generally follows first-order kinetics with respect to drug concentration. Profile *c* corresponds to zero-order kinetics, in which the release process is constant and dependent on time; this kind of profile is desirable for long-term drug delivery systems. Profile *d* represents a stimulus-responsive system in which external changes (such as pH, temperature, magnetic field, etc.) allow controlled release.

III. Experimental Methods

III.1. MESOPOROUS SILICA SYNTHESIS AND FUNCTIONALIZATION

All of the work carried out was based on the hexagonally-ordered fibrous SBA-15[17].

III.1.1. SBA-15 powder synthesis

Materials

Fibrous SBA-15 was synthesized using Pluronics (P123, $PEO_{20}PPO_{70}PEO_{20}$, *Sigma-Aldrich*, Fig. II.3) as a structure directing agent , tetraethyl orthosilicate (TEOS, 98%, *Sigma-Aldrich*, Fig. II.4) as a silica precursor, hydrochloric acid (HCl, 37%, *Sigma-Aldrich*) to control acidity, ethanol (98%, *Sigma-Aldrich*) for washing and distilled water (DIW) as a solvent.

Synthesis was carried out in a 250 ml beaker covered with laboratory film, stirring and heating was carried out on a hotplate magnetic stirrer (IKA® RCT basic). Aging was carried out in pressure reactors consisting of a stainless steel jacket and an internal removable teflon vessel (43 cm^3, 4 vessels per synthesis) in a forced convection oven (Memmert). Filtration was carried out in a 1000 ml Büchner flask. Calcination was done in a ceramic crucible in a muffle furnace (Hobersal).

Procedure

In a typical synthesis, 4 g of P123 are dissolved at 37ºC in 120,8 ml DIW and 3,2 ml HCl, stirring at 350 rpm. After complete dissolution, 9,2 ml of TEOS are added drop by drop and the beaker is covered with laboratory film and left under stirring and heating for 24 h, and then aged for 3 days in Teflon vessels at 100ºC.

The solid product was then filtered and washed three times with DIW and dried for 24 h at room temperature. Removal of the organic template was achieved by calcination in ambient air from room temperature to 550ºC with a heating rate of 1ºC/min and holding time of 6 h at 550ºC, and left to cool.

III.1.2. SBA-15 powder functionalization

As was previously mentioned (see section II.3), organic modification of the surface of SBA-15 enables higher control of release. The experimental protocol for functionalizing SBA-15 is described below:

Materials

SBA-15 was functionalized with (3-Aminopropyl)triethoxysilane (APTES, *Sigma-Aldrich*, Fig. III.1), in anhydrous toluene (*Sigma-Aldrich*).

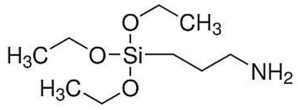

Fig. III.1. Molecular structure of (3-Aminopropyl)triethoxysilane

Functionalization was carried out in a 250 ml three-neck round-bottom flask/reflux column setup, while stirring and heating on a hotplate magnetic stirrer (IKA® RCT basic). Filtration was carried out in a 1000 ml Büchner flask.

Procedure

Functionalization of SBA-15 powders was realized as follows: 1 g of SBA-15 was weighed in the flask which was coupled to the reflux column. Functionalization must be carried out in a humidity-free environment, so an inert gas line (typically Ar) was also coupled to the setup and the system is purged of humidity using a low gas flow during 30 minutes (the gas flow is adjusted so that powder remains motionless). The remaining neck was covered using a rubber plug. See Fig. III.2.

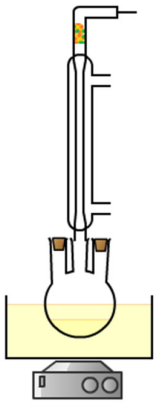

Fig. III.2. Functionalization setup.

After creating an inert atmosphere inside the flask, the gas line was removed and the neck immediately covered using a rubber plug. Functionalization must be carried out in organic media, so 20 ml of anhydrous toluene were added using a syringe while stirring at 300 rpm and heating to 120ºC. Upon reflux, 0,476 ml of APTES were added and the reaction was left between 7 and 8 h.

The flask was then cooled and the solid is filtered and washed three times with ethanol. Powder was dried overnight in an oven at 45ºC.

III.2. MONOLITH PREPARATION AND FUNCTIONALIZATION

Mesoporous silica monoliths with a bimodal pore structure (mesopores and macropores) were prepared using gel-casting procedures, in which SBA-15 particles are entrapped in a cross-linked polyacrylamide macromolecular network; the polymer/particle composition replicates the shape of the model used and the shape remains after polymer network removal.

III.2.1. Monolith preparation

Materials

The elastic hydrogel/particle network was formed using the monomer acrylamide (Ac, 99%, *Sigma-Aldrich,* Fig. III.3), cross linker N-N'-methylene-bisacrylamide (BisAc, 99%, *Sigma-Aldrich*,

Fig. III.4) and initiatior ammonium persulfate $(NH_4)_2S_2O_8$ as a suspension in DIW. Monoliths are prepared with SBA-15 functionalized with APTES. This functionalization is lost after calcination (see section IV.1, TGA results. Monoliths exhibit higher mechanic stability when prepared with functionalized SBA-15 (see section IV.1, mechanical stability results).

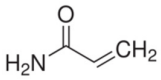

Fig. III.3. Molecular structure of monomer acrylamide.

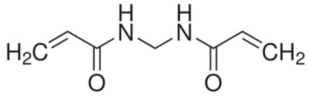

Fig. III.4. Molecular structure of cross-linker N-N'-methylene-bisacrylamide.

Monoliths were prepared in 3 mm i.d. glass tubes placed inside PMMA loaded microcentrifuge tubes that function as a support (see Fig. III.5). Suspension underwent centrifugation in a microcentrifuge (Labnet Spectrafuge 24D) with a maximum capacity of 24 x 1,5/2 ml. Hydrogel hardening and drying were carried out in a forced convection oven (Memmert) and calcination in a ceramic crucible in a furnace.

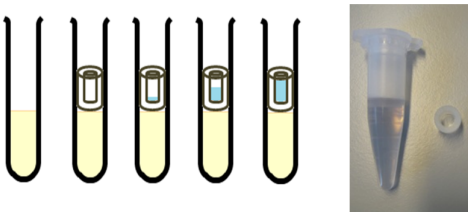

Fig. III.5. Monolith preparation sequence (left); microcentrifuge and glass tubes (left).

Procedure

The weight ratio of monomer, cross-linker and initiator in DIW was 5:0,5:0,05:100, with a weight content of SBA-15 of 2%. Reagents were mixed in a vial and sonicated for 10 minutes to ensure a homogeneous suspension. The suspension was transferred into glass tubes and centrifuged at 3500 rpm for 5 min. Silica particles were packed at the bottom of the tube by centrifugal force and the supernatant was replaced with fresh suspension and centrifuged once again, repeating until the desired height was achieved.

Tubes were capped and cured in an oven at 50ºC for 1 h (monomer and cross-linker polymerization, hydrogel formation) and then uncapped and left at this temperature overnight for hydrogel hardening.

The hard column was dried thoroughly in a vacuum oven at 60ºC and 100 mbar for 48 h, and the glass tubes were removed from inside microcentrifuge tubes and calcined in a ceramic crucible in ambient air from room temperature to 700ºC with a heating rate of 2ºC/min and holding time of 10 h at 700ºC.

After calcination, hard silica monoliths can be easily removed from glass tube models and stored for later use.

Mechanical stability was tested by submerging in PBS for a prolonged period of time. Initial monoliths were lyophilized, weighed and left in PBS for 21 days at 37ºC, then filtered and lyophilized again, to determine mass loss.

III.2.2. Monolith functionalization

Functionalization of monoliths is analogous to powder functionalization, except the monoliths did not undergo stirring but agitation is achieved due to the boiling of toluene (stirring with a magnetic stirrer would crack monoliths). Filtration in this case was carried out on filtration paper.

III.3. MESOPOROUS MATERIAL AND MONOLITH CHARACTERIZATION

Various techniques were applied to characterize the SBA-15 powder and monoliths. Below is a detailed account of each one, along with the conditions used for each case.

III.3.1. Scanning electron microscopy

With scanning electron microscopy (SEM) it's possible to obtain high-resolution images of a sample by scanning the surface with a high-energy electron beam (KeV) in a raster pattern. The topographical image is constructed by analysis of the signal of secondary electrons emitted by the sample's surface upon the action of the high-energy electron beam.

Samples need previous preparation to ensure electrical conductivity; this is achieved by covering the sample with a thin layer of a conducting material (in our case gold was employed) via vacuum sputter coating.

SEM was used to determine the morphology of SBA-15 powder and confirm its fibrous structure, as well as to calculate particle size and distribution. It was also possible to view the structure and morphology of the monolithic silica (particle packing). SEM imaging was carried out on a FEI™ Inspect F50 Scanning Electron Microscope and on a FEI™ Quanta™ Scanning Electron Microscope.

III.3.2. Transmission electron microscopy

By transmitting a beam of electrons through an ultrathin specimen (<200nm), it's possible to obtain a very high-resolution image due to the electron-sample interaction. Part of the incident beam is transmitted, another part is dispersed and a fraction of the beam interacts with the sample giving way to a series of different interactions that are useful for obtaining information on the sample, such as morphology and crystalline structure.

Transmission electron microscopy (TEM) sample preparation involves dissolving solid silica samples in non-polar media (ethanol) and sonicating to ensure a better dispersion. A drop of this suspension is deposited on a mesh grid and left to dry, while the particles remain.

TEM was used to study SBA-15 powder pore size and distribution. TEM imaging was carried out on a FEI™ Tecnai F30 Microscope.

III.3.3. Small-angle X-Ray diffraction

Small-angle X-ray diffraction (SA-XRD) consists of analyzing diffraction of X-rays to obtain information on the crystallographic phases of a sample. The wavelength of X-rays is of the same order of magnitude as interatomic distances within crystalline materials, thus it is possible for X-rays to be diffracted and crystal diffraction patterns can be obtained.

SA-XRD patterns obtained were employed to confirm the characteristic hexagonal structure of SBA-15, for powder and monoliths alike. CuKα radiation (λ = 1,5406 Å, 40kV) in the range of 0,6 to 10,0º (2Θ) was used (Philips™ X'Pert Plus, Faculty of Pharmacy, Universidad Complutense de Madrid).

III.3.4. Nitrogen adsorption

Adsorption occurs when a gas or liquid solute (adsorbate) accumulates on the surface of a solid (adsorbent). In the case of a gas adsorbate, gas molecules accumulate on the solid surface to form an initial monolayer and repeated multilayers as the partial pressure of the gas increases. Techniques based on physical adsorption allow us to determine properties of micro and mesoporous materials such as pore shape and size, specific surface area and specific pore volume.

By means of nitrogen adsorption evaluations, it was possible to determine properties of SBA-15 powder and monoliths based on the Brunauer-Emmett-Teller (BET) and Barret-Joyner-Halenda (BJH) theories, namely specific surface area, specific pore volume and pore size distributions, as well as pore structure via analysis of adsorption isotherms. Measurements were carried out (after previous degasification in vacuum at 473 K for 3 h) at 77K for 8 hours for unfunctionalized materials and 3 hours for functionalized materials, on a surface area and pore size analyzer (Micromeritics™ Tristar 3000).

III.3.5. Mercury porosimetry

Porosimetry is useful when determining macropore properties. A non-wetting liquid, specifically mercury, is forced to intrude the pore structure of as-synthesized monoliths that have been previously degassed. Roughly, the volume of mercury that intrudes into the samples due to an increase of pressure is equivalent to the pore volume in an associated size range depending on the pressure employed.

Mercury porosimetry was used to determine total and interstitial porosity and interstitial pore size of SBA-15 monoliths. Analysis was carried out on a mercury intrusion porosimeter (Micromeritics™ AutoPore IV).

III.3.6. Thermogravimetric analysis

Thermogravimetric analysis (TGA) enables us to determine the composition of a sample by continuously increasing the sample temperature in a controlled environment and recording the mass loss, which is associated to the decomposition of the phases within the sample. Materials constituting the sample decompose at different temperatures, making a qualitative and quantitative analysis possible by differentiation of the thermogram obtained (weight vs. temperature).

TGA was employed to confirm the presence of APTES and cefuroxime in the sample. Measurements were carried out using a heating rate of 5ºC/min until 900ºC using a N_2 flow of 15ml/min (TA Instruments™ Thermogravimetric Analyzer).

III.3.7. UV-Visible spectroscopy

UV-Visible spectroscopy (UV-Vis) is a colorimetric technique widely used to identify organic and inorganic species within a sample.

UV-Vis was used for two purposes: as a tool to determine the amount of cefuroxime loaded onto SBA-15 powders and monoliths and to study the release mechanisms of said materials.

UV-Vis measurements were carried out on an UV-Vis spectrophotometer (8453 UV-Visible, Agilent™) at 278 nm, which is the characteristic absorbance wavelength of cefuroxime. The equipment consists of a light source of two lamps (wavelength range from 190 to 1100 nm), a monochromator to separate different wavelengths and a detector.

III.4. CEFUROXIME LOADING AND RELEASE

Drug delivery experiments were conducted on four different samples, namely unfunctionalized and functionalized SBA-15 powders (P-SBA-15 and P-SBA-15') and monoliths (M-SBA-15 and M-SBA-15', respectively).

III.4.1. Cefuroxime loading

Loading of cefuroxime sodium salt (CEF, *Sigma*-Aldrich, Fig. III.6) onto SBA-15 powders and monoliths was accomplished using the same technique for both materials, in order to establish differences regarding the amount of drug adsorbed onto the mesoporous material, specifically due to the difference in macroscopic configuration.

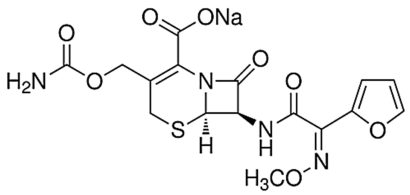

Fig. III.6. Molecular structure of Cefuroxime Sodium Salt (CEF).

Prior to loading, it is necessary to dehydrate the pores of the material, which is done by lyophilization (Telstar Cryodos Lyophilizer).

Previous work carried out by members of the NFP group have demonstrated that loading of cefuroxime in a 1:2 proportion with respect to the mesoporous material yields the highest possible loads; for this reason this proportion was chosen as a base for cefuroxime loading (Carmona and Balas, unpublished data). The corresponding volume of a solution of cefuroxime in DIW with a concentration of 5 mg/ml was added onto approximately 20 mg of SBA-15 powders and monoliths alike immediately after lyophilizing in a glass vial. For monolith loading, the vial underwent moderate stirring (to avoid monolith damage) in an orbital shaker (IKA®KS 130 Control) at 230 rpm and room temperature; for powder loading the vial was

placed on a roller and tilt mixer (SELECTA Movil-Rod). After 24 hours, the powders and monoliths were filtered on laboratory filter paper and washed once with 1ml DIW, and left to dry in ambient conditions for another 24 hours.

III.4.2. Cefuroxime release

Cefuroxime release mechanisms from SBA-15 powders and monoliths were determined using UV-Vis spectroscopy in a continuous mode (see Fig. III.7). It was possible to measure the absorbance of the release media in order to monitor cefuroxime release. Measurements were carried out at controlled time intervals at the characteristic absorbance wavelength of cefuroxime. Absorbance measurements were carried out in the UV-Vis spectrophotometer described in section III.3.7.

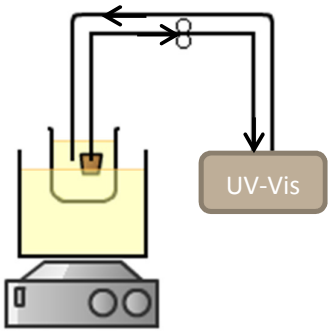

Fig. III.7. Continuous-measurement release setup.

The setup consists of a circuit comprising polyurethane piping and a peristaltic pump that directs the release media from the initial release vial through a quartz cuvette where absorbance measurements are executed and back to its original vial. The release vial was placed inside an oil bath on a heating plate (IKA® RCT basic). Release media must be filtered prior to entering the cuvette as solid particles would result in light scattering and, therefore, erratic measurements. For this a stainless steel filter was placed on the pipe entrance.

Release experiments were conducted as follows: approximately 20 mg of cefuroxime-loaded SBA-15 powder or a cefuroxime-loaded monolith were placed in the glass vial. The filter and pipe exit were both placed inside the vial and set in place with laboratory film which also seals the vial to prevent evaporation of release media. After the setup is complete, 5 ml of release media were added using a syringe. A 1X phosphate buffered saline solution (PBS) was used as a release media, at 37ºC in order to simulate physiological conditions as closely as possible. Agitation was achieved due to the flow of release media, as using magnetic stirrers would crack monoliths.

Time-based measurement specifications are as follows: the first measurement was conducted 15 s after the program was initialized (program should be initialized immediately after PBS is added to loaded mesoporous material), then every 60 s until 1000 s. After this, measurements were carried out with an increment of 10% in time with respect to the previous measurement given that release tends to be slower after the initial burst. Measurements are recorded for a maximum of $1{,}8 \cdot 10^5$ s (approximately 2 d).

IV. Results and Discussion

IV.1. MONOLITH AND MESOPOROUS MATERIALS CHARACTERIZATION

Powder and monolithic SBA-15 were characterized using the techniques detailed in section III.3. The results obtained are explained in this section.

IV.1.1. SEM Imaging

The fibrous morphology of P-SBA-15 and M-SBA-15 can be clearly seen in **SEM** micrographs (Fig. IV.1). An image analysis to determine particle dimensions resulted in diameters between 4,5 and 7,5µm and lengths between 75 and 105µm, with a highly irregular distribution. The final micrograph shows how SBA-15 particles agglomerate to form the solid monolithic structure (see Fig. IV.2 for photographs of the final products).

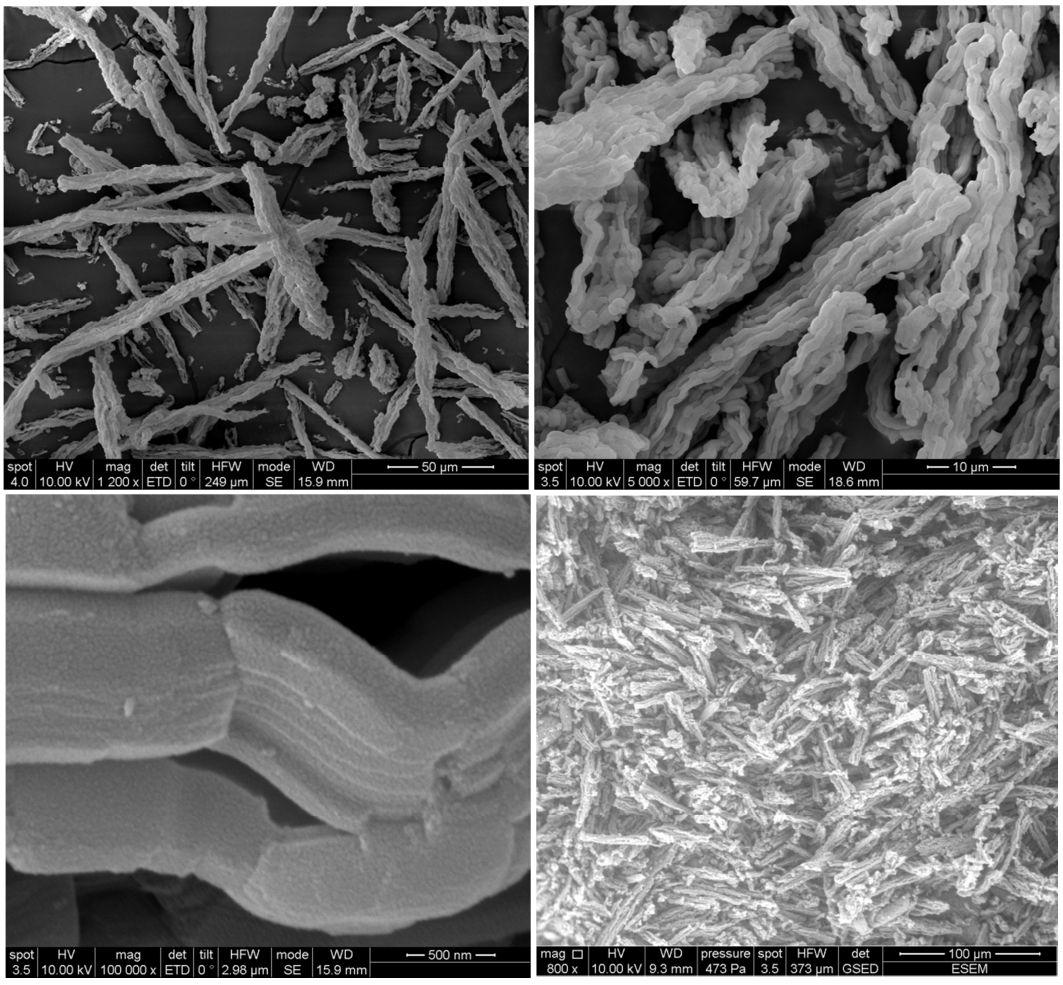

Fig. IV.1. SEM micrographs of synthesized fibrous SBA-15. The final micrograph is an image of a longitudinal section of a monolith.

Fig. IV.2. Calcined monoliths.

IV.1.2. TEM Imaging

TEM micrographs (Fig. IV.3) of P-SBA-15 show well-defined pores and a uniform pore size distribution. An image analysis to determine pore size resulted in an average of 5,60±0,12 nm. The characteristic hexagonal pore structure of SBA-15 can be clearly seen on the inset micrograph.

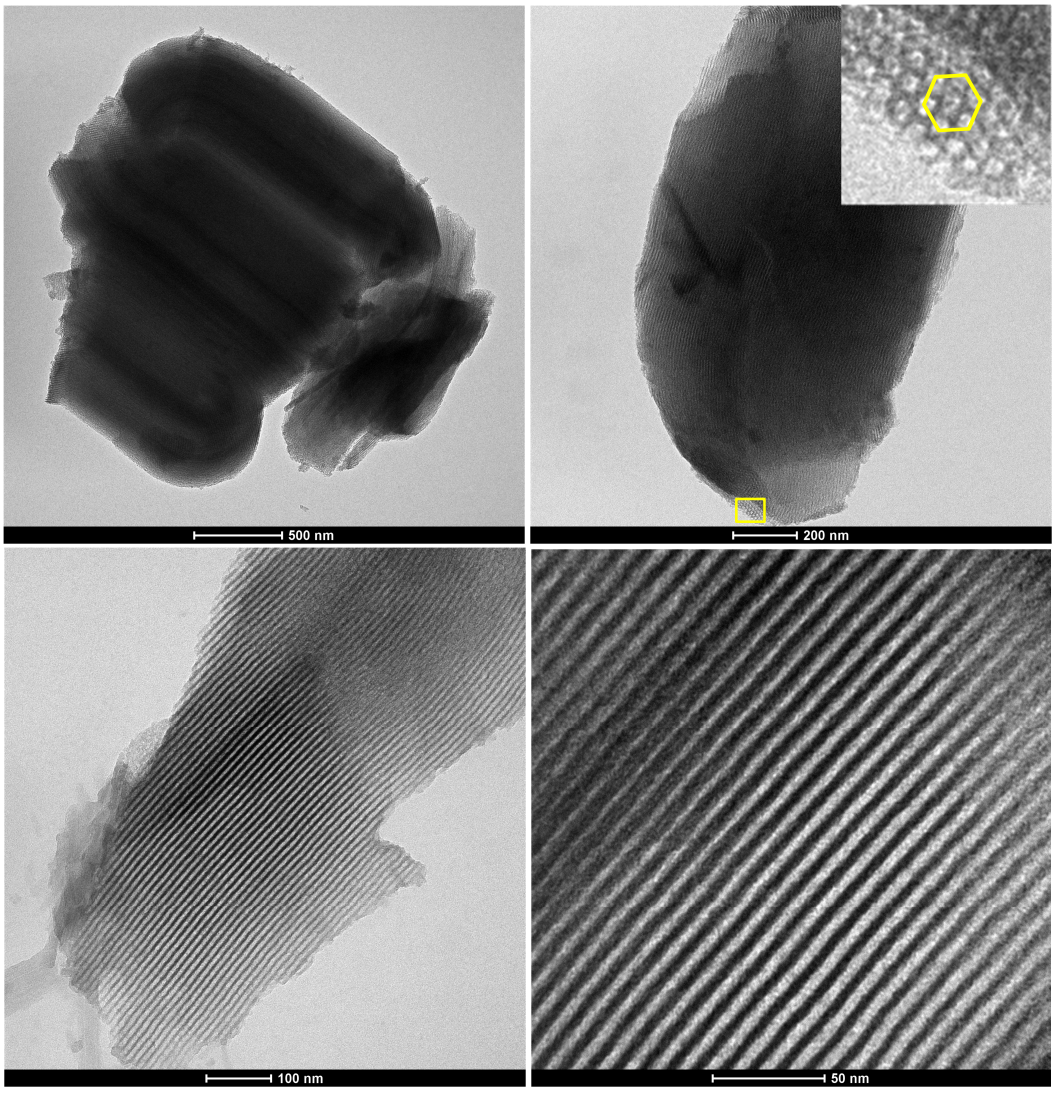

Fig. IV.3. TEM micrographs of SBA-15 powders.

IV.1.3. SA-XRD Analysis

SA-XRD spectra for P-SBA-15 (Fig. IV.4) show three clear peaks which can be indexed as (1 0), (1 1) and (2 0) reflections. These are characteristic of the reflections of a 2D hexagonal symmetry (*p6mm*).

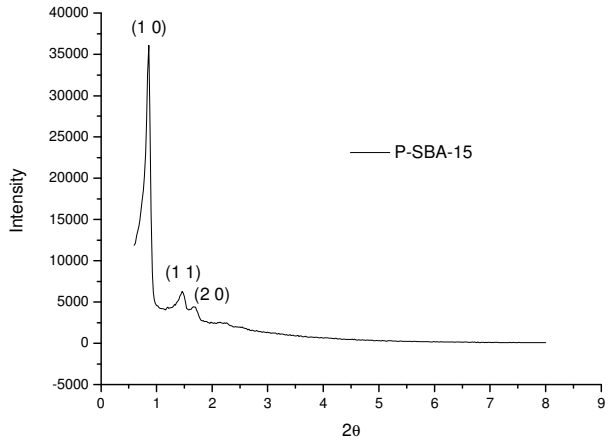

Fig. IV.4. Small-angle X-Ray Diffraction spectrum for P-SBA-15. Three characteristics peaks of a hexagonally-ordered structure are shown.

IV.1.4. Nitrogen adsorption analysis

Materials pore shape and size, specific surface area and specific pore volume were determined by **nitrogen adsorption** evaluations. Adsorption isotherms are functions that relate the amount of adsorbate adsorbed at equilibrium, to the pressure of the adsorbate in the gas phase, at a constant temperature. Adsorption of a gas depends, amongst other things, on the porous structure of the adsorbant. Therefore it is possible to determine additional information on pore shape by adsorption isotherm analysis.

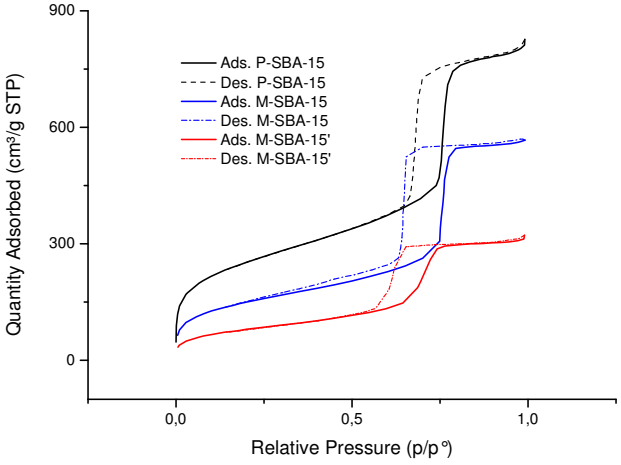

Fig. IV.5. Adsorption/desorption isotherms.

According to the IUPAC, there are six types of physical adsorption isotherms, and four types of hysteresis[43]. In Fig. IV.5, the adsorption isotherms of P-SBA-15 and the monolithic forms are shown. The isotherms can be classified as type V, which are associated to mesoporous structures. Hysteresis in corresponds to the type H-1, which is characteristic of well-defined cylindrical pores and uniform pore size distribution. This information confirms the information collected from TEM micrographs in which an ordered and uniform mesoporous structure was observed.

Using the BET theory model, the specific surface areas of each material were determined. Pore sizes and specific pore volume were calculated using the BJH theory. The table below summarizes these properties.

Table IV.1. SBA-15 powder and monolith properties determined by N_2 adsorption.

	P-SBA-15	M-SBA-15	M-SBA-15'
Pore shape	Cylindrical	Cylindrical	Cylindrical
Pore size (nm)	6,9	6,8	6,7
Specific surface area (m^2/g)	914,6	547,0	294,4
Specific pore volume (cm^3/g)	1,16	0,90	0,50

P-SBA-15: Powder SBA-15, M-SBA-15: Monolithic SBA-15; M-SBA-15': APTES modified monolithic SBA-15

There is a reduction in specific surface area and pore volume *after functionalization*, due to the incorporation of organic moieties. It has been suggested that this reduction can be attributed to the blockage of much smaller pores (>2nm) that may be present with a broad distribution within the mesoporous materials[44]. The grafting of organic moieties modifies the silica surface, making it difficult for nitrogen molecules form the monolayer necessary for N_2 adsorption measurements on the material surface. Upon applying the aforementioned mathematical models to determine specific surface area and pore volume, a reduction is obtained due to the direct dependency of the models to the amount of N_2 adsorbed. As was detailed in sections III.1 and III.2, materials were functionalized with (3-Aminopropyl)thriethoxysilane (APTES). The approximate size of this molecule is 1,3nm in length and 0,7 nm in diamterer[45].

The reduction in specific surface area and pore volume between the *powder* and *monolithic* form of SBA-15 can be attributed to the incorporation of an additional Si layer on the surface of the material, aside from the pore blockage previously mentioned. As was explained in section III.2, monoliths are prepared with previously functionalized SBA-15 powders due to the fact that they showed a higher mechanical stability than those prepared with unfunctionalized SBA-15 (see section IV.1.6). Upon calcination during monolith preparation, the organic tails of APTES are lost, but the additional Si atom remains within the structure. Further functionalization (M-SBA-15') would result in an even lower specific surface area and pore volume.

The change in mesopore size however is hardly significant, suggesting that grafting of small organic moieties on larger pores does not affect their size, but again confirming that blockage of micropores with the same moieties is possible.

IV.1.5. Mercury porosimetry analysis

Further characterization of the porous structure of SBA-15 *monoliths* was carried out by **mercury intrusion porosimetry** evaluations. Due to the shape of SBA-15 particles, monoliths have a bimodal array of pores: the characteristic mesopores of SBA-15 and macropores in the range of microns that correspond to the interstitial sites formed within the monolith (see section IV.1.1). Fig. IV.6 shows the intrusion and extrusion curves of M-SBA-15 and M-SBA-15'. Pore sizes and interstitial and total porosity of monoliths are presented in the table below.

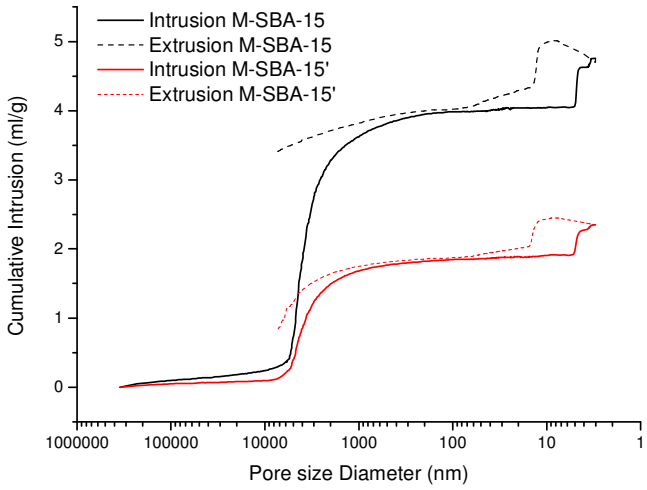

Fig. IV.6. Hg porosimetry of unmodified (SBA-15) and modified (SBA-15+APTES) monoliths.

Interstitial pores are larger than the mesopores and therefore hold more mercury than particle pores. Moreover, unfunctionalized monoliths will hold more mercury than their functionalized counterparts; total intrusion volume for M-SBA-15 was 4,756 ml/g, while for M-SBA-15' intrusion reached 2,348 ml/g.

Two pore sizes are discernible in Fig. IV.6 (intrusion curve), corresponding to the pore distribution described above.

Table IV.2. SBA-15 monolith properties determined by Hg porosimetry.

	M-SBA-15	M-SBA-15'
Interstitial pore size (μm)	3,43	3,19
Interstitial porosity (%)	47,6	47,6
Total porosity (%)	84,5	83,4

Interstitial pores of M-SBA-15 are slightly larger than those of M-SBA-15', and total porosity is reduced after functionalization, most likely due to micropore blockage as was described in the previous section. The slight decrease in total porosity is also due to pore blockage.

IV.1.6. Thermogravimetric Analysis

Organic modification of SBA-15 powders and monoliths was confirmed via **TGA**. The figure below show TGA and derivative TGA curves of modified and unmodified SBA-15 powders and monoliths. A peak is clearly discernible in the derivative curve for the temperature range of 400 to 600ºC[46], which is attributed to the decomposition of APTES in a nitrogen atmosphere. This indicates effective surface modification.

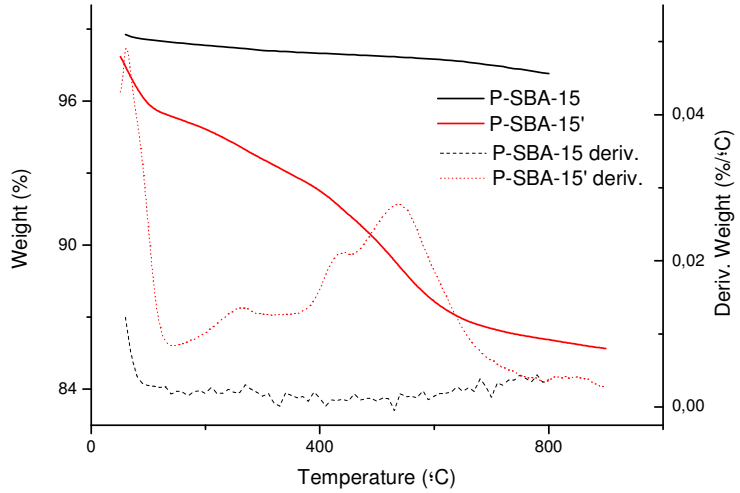

Fig. IV.7. TGA spectra for APTEs-modified SBA-15 powders.

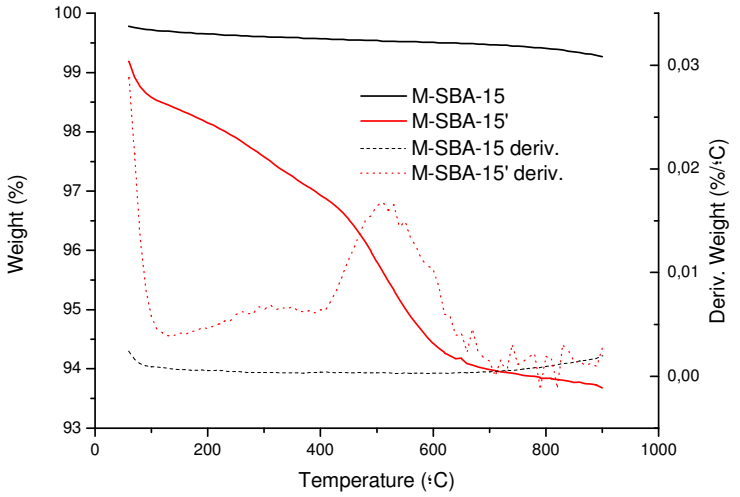

Fig. IV.8. TGA spectra for APTES-modified SBA- monoliths.

Monoliths showed a 3,2% in weight of effective surface modification versus 5,9% for powders. Monoliths yield a lower silanization given that they are prepared using previously functionalized SBA-15 powders. Although the organic groups of APTES are lost after monolith calcination, a decrease in the hydroxyl sites available for functionalization with respect to the

powder counterpart is possible, resulting in a less effective organic modification. Moreover, diffusion of the functionalization agents to the interior of monoliths is difficult given their macroscopic morphology.

IV.1.7. Mechanical stability assays

Mechanical stability of monoliths was determined by calculating the difference in mass for monoliths left for 21 days in PBS at 37ºC. Mass loss for SBA-15 monoliths prepared with unfunctionalized material was of 37,4%, while for those prepared with functionalized SBA-15 mass loss was 4,2%. Monoliths prepared with functionalized SBA-15 proved to be more resistant to dissolution in aqueous media, for this reason they were chosen as matrices for drug delivery experiments.

IV.2. CEFUROXIME RELEASE

IV.2.1. Cefuroxime loading

Materials under study (P-SBA-15, P-SBA-15', M-SBA-15 and M-SBA-15') were soaked during 24h in a solution of the model antibiotic (cefuroxime sodium salt, CEF) to entrap drug molecules within the available pores (see section III.4).

Effective uptake of CEF was confirmed by TGA (see Fig. IV.9-Fig. IV.11). A peak is observed in the derivative curve from 100 to 110ºC which corresponds to elimination of water from samples. From 200 to 300ºC, a peak is discernible which can be attributed to decomposition of cefuroxime. As was previously mentioned, the peak in the range from 400 to 600ºC corresponds to the decomposition of APTES in the sample.

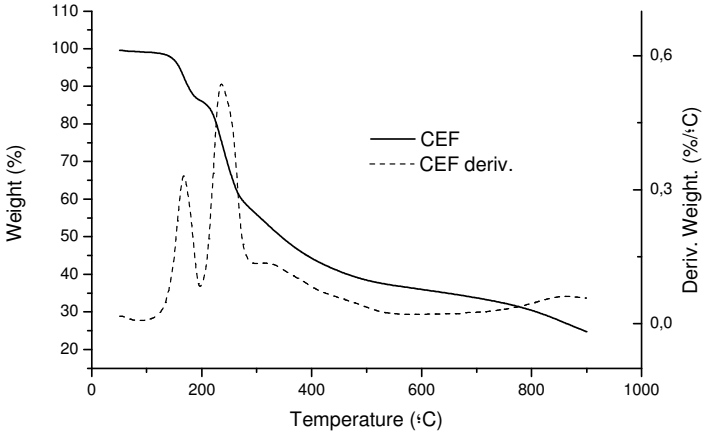

Fig. IV.9. TGA spectra for cefuroxime sodium salt.

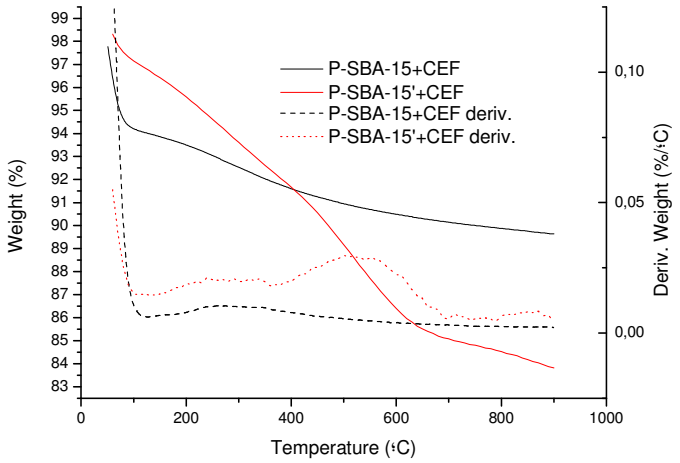

Fig. IV.10. TGA spectra for cefuroxime-loaded powders.

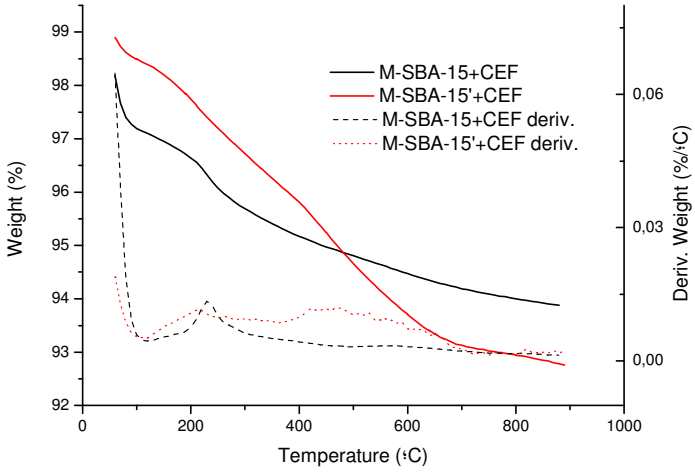

Fig. IV.11. TGA spectra for cefuroxime-loaded monoliths.

According to TGA, CEF was effectively loaded onto SBA-15 powders and monoliths in the following ascending order, represented as a weight percentage of CEF in SBA-15: M-SBA-15 (1,07%), M-SBA-15' (1,20%), P-SBA-15 (1,24%) and P-SBA-15' (2,27%).

Loading of CEF was calculated by a mass balance between initial antibiotic solution and supernatant after 24h of loading; were determined by UV-Vis spectroscopy. Drug content of the different matrices studied are shown in the table below.

Table IV.3. Cefuroxime uptake on SBA-15 powders and monoliths.

Material	% wt with respect to Q_0	% wt with respect to SBA-15 wt
P-SBA-15	17,59	8,80
P-SBA-15'	18,64	9,31
M-SBA-15	14,80	7,40
M-SBA-15'	16,93	8,46

Q_0: mass of cefuroxime in initial loading solution

TGA and UV-Vis calculations indicate that the material with the highest CEF uptake is P-SBA-15'. In contrast to the unfunctionalized P-SBA-15, a higher loading is possible due to amino groups readily available on the P-SBA-15' surface which increase the drug-surface interaction. This increase is due to possible ionic interactions between protonated amino groups and the carboxyl group of CEF, versus the weaker hydrogen bonds that are formed between the carboxyl group and the hydroxyl group available on unfunctionalized surfaces[10].

Uptake of CEF on *monoliths* is lower than that of the powder counterparts. Powders exhibit a higher surface area to volume ratio and are therefore in higher contact with the initial loading solution; diffusion of said solution through the monolith may prove difficult.

IV.2.2. Cefuroxime release

Release kinetics are studied as a function of time, and for the case of a water-soluble drug incorporated in a matrix, it is assumed that release is due to diffusion[35]. Generally, for mesoporous materials, release profiles tend to exhibit and initial burst release followed by a more controlled release pattern[37]. In the present study, variations in this abrupt release are due to the macroscopic morphology of the release matrix (powder and monolithic materials).

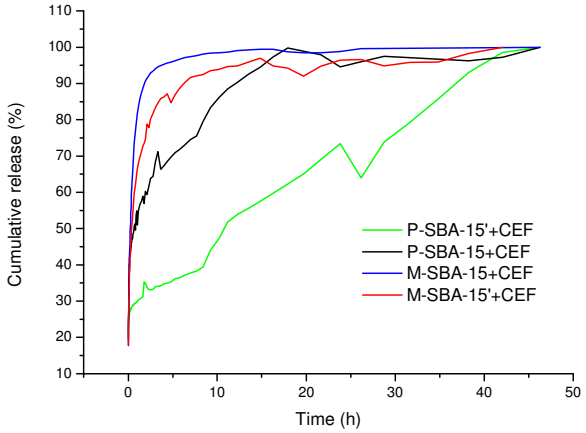

Fig. IV.12. Cumulative release profiles of CEF from materials under study.

According to Fig. IV.12, release of CEF from both unfunctionalized and functionalized monoliths exhibits an initial burst release followed by a more controlled delivery. This behavior is the result of CEF diffusing from the macropores of monoliths. A large amount of the total CEF loaded may be entrapped within the macropores, creating a drug reservoir. Due to the

larger size of these pores, diffusion to the release media is easier and a large amount of material is delivered abruptly. A more controlled release can be observed for M-SBA-15' in contrast to M-SBA-15 after the initial burst. This is the result of functionalization of mesopores, which makes drug diffusion towards the release media more difficult due to the ionic interactions between said molecules and amino groups on the mesopore surface.

Fig. IV.12 also confirms that cefuroxime release from powders is slower than from monolithic counterparts. As there are no large drug reservoirs, initial burst release is small and can be attributed to desorption of drug molecules located on mesopore entrances. A more controlled release from P-SBA-15' as compared to P-SBA-15 is expected for the same reason described above; functionalization will result in retention of drug molecules yielding slower delivery.

Cumulative profiles can be used to accomplish dissolution studies for in-vitro release. Release kinetics parameters were calculated in order to establish a comparison between release profiles, based on the cumulative adsorption plot. The diffusion model chosen to study the delivery of CEF from each system assumes extraction of the drug from the pores of the matrix by means of contact with the release media; the drug dissolves slowly into the fluid phase and diffuses from the system along the pores. Higuchi developed a theoretical model that can be applied to these studies. The equation that is used to predict the release rate is:

$$Q = kt^{1/2} \quad \text{...(Ec. IV.1)}$$

where Q is the amount of drug released after time t and k is the release constant. The amount of drug released was plotted against the square root of time and the data was fitted to a linear regression. The threshold limit for the valid application of the Higuchi model was adjusted to the time when said fitting had the highest possible regression coefficient. This adjustment offers information on the kinetic of release as well as the time for which delivery follows this particular model.

Table IV.4. Kinetic constants for the systems under study.

Material	k	r^2	Time limit (h)
P-SBA-15	16,203	0,95	17,9
P-SBA-15'	10,265	0,95	46,25
M-SBA-15	63,637	0,96	1,61
M-SBA-15'	40,988	0,96	2,52

k: kinetic constant, r^2: regression coefficient

As is expected, the matrix with the highest kinetic constant is M-SBA-15, followed by M-SBA-15', P-SBA-15 and with P-SBA-15' exhibiting the slowest release. This again indicates that the monolithic form yields a faster delivery, and functionalization enables more control over kinetics. This trend can also be observed in the time limits for modeled release, being P-SBA-15' the matrix that follows the Higuchi model for the longest period of time. After the time limit, it is assumed that quasi-equilibrium has been reached and delivery is very slow.

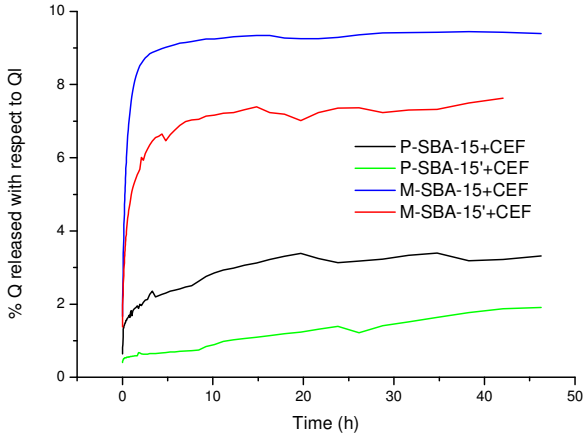

Fig. IV.13. Absolute release profiles. Release calculated with respect to effective CEF loaded (Q_l).

Fig. IV.13 shows effective release with respect to CEF loaded onto each material. The material with the highest amount of drug released is M-SBA-15, with 9,4% of release. This can be attributed to the fact that there are weak interactions between drug molecules and surface, as the material is unfunctionalized. Moreover, there are drug reservoirs within the macropores that represent a large part of the total amount of drug loaded; release from these reservoirs is thought to be faster as diffusion from said macropores is less difficult than diffusion from mesopores.

M-SBA-15' exhibits a release profile similar to that of its unfunctionalized counterpart; however less drug is delivered to the release media (7,6%). As was previously mentioned, functionalization enables a more controlled delivery of the drug, therefore a slower release is expected. It is possible that release has not yet reached equilibrium after the set experimental release time, and more drug molecules can be delivered to the release media. However, it is commonly observed that the complete desorption of the drug is seldom found[37], due to the equilibrium achieved at the end of the desorption process that results in partial retention of the drug within the delivery matrix. In the case of functionalized matrices this is more evident due to stronger drug-surface interactions.

Powder matrices exhibit less CEF delivery than monolith matrices (1,9% for P-SBA-15' and 3,3% for P-SBA-15). In spite of higher loadings in powder matrices, delivery is slower because there are no large (macroporous) reservoirs that release high quantities of drugs in a short period of time; drug release depends solely on desorption of drug located inside the mesopores of SBA-15 and near the surfaces of the pore entrance. The matrix P-SBA-15' exhibits a slower release due to retention of drug molecules as an effect of ionic interaction between the amino groups of APTES and the carboxyl groups of CEF; the portions of the curve after burst release are parallel in the case of P-SBA-15' and M-SBA-15, indicating similar release kinetics for the functionalized matrices.

V. Conclusions

An effective synthesis of fibrous SBA-15 powder with an ordered hexagonal mesoporous structure was achieved, as well as functionalization of the resulting mesoporous silica with the aminosilane APTES.

Successful functionalization of SBA-15 enabled preparation of mechanically stable monolithic SBA-15 that exhibited a bimodal pore structure, with macropores in the range of microns and the corresponding characteristic mesopores, confirmed by intrusion analysis, whereas without surface functionalization stable monolithic structures could not be prepared. Functionalization of said monoliths was also achieved however in a lower degree than the powder counterparts, due to difficult diffusion of the functionalizing agent to the interior of the monolith.

Loading of a model antibiotic, namely cefuroxime sodium salt onto amino-functionalized and unfunctionalized SBA-15 powders and monoliths yielded higher loadings for powders, as well as higher loadings for functionalized matrices, given the strong ionic interaction that occurs between amino groups and carboxyl groups present in cefuroxime.

Controlled drug delivery studies of cefuroxime from amino-functionalized and unfunctionalized SBA-15 powders and monoliths were conducted, resulting in a faster release from monolithic matrices than powder counterparts due to the bimodal porous structure in which macropores can function as initially fast-releasing drug reservoirs. Furthermore, a more controlled release was achieved via functionalization with aminosilanes.

VI. References

1 Rouquerol, J. *et al.* Recommendations for the characterization of porous solids. *Pure & Appl. Chem.* **66**, 1739-1758, doi:10.1351/pac199466081739 (1994).

2 Chiola, V., Ritsko, J. E. & Vanderpool, C. D. Process for producing low-bulk density silica. (1971).

3 Di Renzo, F., Cambon, H. & Dutartre, R. A 28-year-old synthesis of micelle-templated mesoporous silica. *Microporous Materials* **10**, 283-286 (1997).

4 Yanagisawa, T., Shimizu, T., Kuroda, K. & Kato, C. The Preparation of Alkyltriinethylaininonium–Kaneinite Complexes and Their Conversion to Microporous Materials. *Bulletin of the chemical society of Japan* **63**, 988-992, doi:10.1246/bcsj.63.988 (1990).

5 Kresge, C. T. *et al. M41S: A new family of mesoporous molecular sieves prepared with liquid crystal templates*. Vol. 92 (Elsevier Science Publ B V, 1995).

6 Yang, P., Zhao, D., Margolese, D. I., Chmelka, B. F. & Stucky, G. D. Block Copolymer Templating Syntheses of Mesoporous Metal Oxides with Large Ordering Lengths and Semicrystalline Framework. *Chemistry of Materials* **11**, 2813-2826, doi:10.1021/cm990185c (1999).

7 Zhao, D. *et al.* Triblock Copolymer Syntheses of Mesoporous Silica with Periodic 50 to 300 Angstrom Pores. *Science* **279**, 548-552, doi:10.1126/science.279.5350.548 (1998).

8 Melde, B. J., Holland, B. T., Blanford, C. F. & Stein, A. Mesoporous Sieves with Unified Hybrid Inorganic/Organic Frameworks. *Chemistry of Materials* **11**, 3302-3308, doi:10.1021/cm9903935 (1999).

9 Yang, P., Zhao, D., Margolese, D. I., Chmelka, B. F. & Stucky, G. D. Generalized syntheses of large-pore mesoporous metal oxides with semicrystalline frameworks. *Nature* **396**, 152-155 (1998).

10 Song, S. W., Hidajat, K. & Kawi, S. Functionalized SBA-15 Materials as Carriers for Controlled Drug Delivery: Influence of Surface Properties on Matrix−Drug Interactions. *Langmuir* **21**, 9568-9575, doi:10.1021/la051167e (2005).

11 Trewyn, B. G., Giri, S., Slowing, I. I. & Lin, V. S. Y. Mesoporous silica nanoparticle based controlled release, drug delivery, and biosensor systems. *Chemical Communications*, 3236-3245 (2007).

12 Ma, Y. *et al.* Large-pore mesoporous silica spheres: synthesis and application in HPLC. *Colloids and Surfaces A: Physicochemical and Engineering Aspects* **229**, 1-8, doi:10.1016/j.colsurfa.2003.08.010 (2003).

13 Ryoo, R., Joo, S. H., Kruk, M. & Jaroniec, M. Ordered Mesoporous Carbons. *Advanced Materials* **13**, 677-681 (2001).

14 Schüth, F. Non-siliceous Mesostructured and Mesoporous Materials†. *Chemistry of Materials* **13**, 3184-3195, doi:10.1021/cm011030j (2001).

15 Beck, J. S. *et al.* Molecular or Supramolecular Templating: Defining the Role of Surfactant Chemistry in the Formation of Microporous and Mesoporous Molecular Sieves. *Chemistry of Materials* **6**, 1816-1821, doi:10.1021/cm00046a040 (1994).

16 Vinu, A., Mori, T. & Ariga, K. New families of mesoporous materials. *Science and Technology of Advanced Materials* **7**, 753-771 (2006).

17 Katiyar, A., Yadav, S., Smirniotis, P. G. & Pinto, N. G. Synthesis of ordered large pore SBA-15 spherical particles for adsorption of biomolecules. *Journal of Chromatography A* **1122**, 13-20, doi:10.1016/j.chroma.2006.04.055 (2006).

18 Zhao, D. *et al.* Continuous Mesoporous Silica Films with Highly Ordered Large Pore Structures. *Advanced Materials* **10**, 1380-1385, doi:10.1002/(sici)1521-4095(199811)10:16<1380::aid-adma1380>3.0.co;2-8 (1998).

19 Schmolka, I. R. Polyoxyethylene-polyoxypropylene aqueous gels. (1966).

20 Raman, N. K., Anderson, M. T. & Brinker, C. J. Template-Based Approaches to the Preparation of Amorphous, Nanoporous Silicas. *Chemistry of Materials* **8**, 1682-1701, doi:10.1021/cm960138+ (1996).

21 Nakanishi, K. Pore Structure Control of Silica Gels Based on Phase Separation. *Journal of Porous Materials* **4**, 67-112, doi:10.1023/a:1009627216939 (1997).

22 Hoffmann, F., Cornelius, M., Morell, J. & Fröba, M. Silica-Based Mesoporous Organic–Inorganic Hybrid Materials. *Angewandte Chemie International Edition* **45**, 3216-3251, doi:10.1002/anie.200503075 (2006).

23 Melosh, N. A. *et al.* Molecular and Mesoscopic Structures of Transparent Block Copolymer-Silica Monoliths. *Macromolecules* **32**, 4332-4342 (1999).

24 Feng, P., Bu, X., Stucky, G. D. & Pine, D. J. Monolithic Mesoporous Silica Templated by Microemulsion Liquid Crystals. *J. Am. Chem. Soc.* **122**, 994-995 (2000).

25 Melosh, N. A., Davidson, P. & Chmelka, B. F. Monolithic Mesophase Silica with Large Ordering Domains. *Journal of the American Chemical Society* **122**, 823-829, doi:10.1021/ja992801b (2000).

26 Minakuchi, H., Nakanishi, K., Soga, N., Ishizuka, N. & Tanaka, N. Octadecylsilylated Porous Silica Rods as Separation Media for Reversed-Phase Liquid Chromatography. *Analytical Chemistry* **68**, 3498-3501, doi:10.1021/ac960281m (1996).

27 Sun, Z. *et al.* Hierarchically Ordered Macro-/Mesoporous Silica Monolith: Tuning Macropore Entrance Size for Size-Selective Adsorption of Proteins. *Chemistry of Materials* **23**, 2176-2184, doi:10.1021/cm103704s (2011).

28 Amatani, T., Nakanishi, K., Hirao, K. & Kodaira, T. Monolithic Periodic Mesoporous Silica with Well-Defined Macropores. *Chemistry of Materials* **17**, 2114-2119, doi:10.1021/cm048091c (2005).

29 Leventis, N. *et al.* Polymer nano-encapsulation of templated mesoporous silica monoliths with improved mechanical properties. *Journal of Non-Crystalline Solids* **354**, 632-644, doi:10.1016/j.jnoncrysol.2007.06.094 (2008).

30 Smått, J.-H., Schunk, S. & Lindén, M. Versatile Double-Templating Synthesis Route to Silica Monoliths Exhibiting a Multimodal Hierarchical Porosity. *Chemistry of Materials* **15**, 2354-2361, doi:10.1021/cm0213422 (2003).

31 Liang, C., Dai, S. & Guiochon, G. Use of gel-casting to prepare HPLC monolithic silica columns with uniform mesopores and tunable macrochannels. *Chemical Communications*, 2680-2681 (2002).

32 Vasiliev, P. O., Shen, Z., Hodgkins, R. P. & Bergström, L. Meso/Macroporous, Mechanically Stable Silica Monoliths of Complex Shape by Controlled Fusion of Mesoporous Spherical Particles. *Chemistry of Materials* **18**, 4933-4938, doi:10.1021/cm061205v (2006).

33 Sachse, A. *et al.* Functional silica monoliths with hierarchical uniform porosity as continuous flow catalytic reactors. *Microporous and Mesoporous Materials* **140**, 58-68, doi:10.1016/j.micromeso.2010.10.044 (2011).

34 Paolino, D., Fresta, M., Sinha, P. & Ferrari, M. in *Encyclopedia of Medical Devices and Instrumentation* (ed John G. Webster) 437-495 (John Wiley & Sons, Inc., 2006).

35 Costa, P. & Sousa Lobo, J. M. Modeling and comparison of dissolution profiles. *European Journal of Pharmaceutical Sciences* **13**, 123-133, doi:10.1016/s0928-0987(01)00095-1 (2001).

36 Farokhzad, O. C. & Langer, R. Impact of Nanotechnology on Drug Delivery. *ACS Nano* **3**, 16-20, doi:10.1021/nn900002m (2009).

37 Vallet-Regí, M., Balas, F. & Arcos, D. Mesoporous Materials for Drug Delivery. *Angewandte Chemie International Edition* **46**, 7548-7558, doi:10.1002/anie.200604488 (2007).

38 Hudson, S. P., Padera, R. F., Langer, R. & Kohane, D. S. The biocompatibility of mesoporous silicates. *Biomaterials* **29**, 4045-4055 (2008).

39 Izquierdo-Barba, I., Martinez, Á., Doadrio, A. L., Pérez-Pariente, J. & Vallet-Regí, M. Release evaluation of drugs from ordered three-dimensional silica structures. *European Journal of Pharmaceutical Sciences* **26**, 365-373, doi:10.1016/j.ejps.2005.06.009 (2005).

40 Vallet-Regí, M., Doadrio, J. C., Doadrio, A. L., Izquierdo-Barba, I. & Pérez-Pariente, J. Hexagonal ordered mesoporous material as a matrix for the controlled release of amoxicillin. *Solid State Ionics* **172**, 435-439, doi:10.1016/j.ssi.2004.04.036 (2004).

41 Doadrio, J. C. *et al.* Functionalization of mesoporous materials with long alkyl chains as a strategy for controlling drug delivery pattern. *Journal of Materials Chemistry* **16**, 462-466 (2006).

42 Doadrio, A. L. *et al.* Mesoporous SBA-15 HPLC evaluation for controlled gentamicin drug delivery. *Journal of Controlled Release* **97**, 125-132, doi:10.1016/j.jconrel.2004.03.005 (2004).

43 Sing, K. S. W. *et al.* Reporting Physisorption Data for Gas/Solid System with Special Reference to the Determination of Surface Area and Porosity. *Pure & Appl. Chem.* **57**, 603-619 (1985).

44 Ryoo, R., Ko, C. H., Kruk, M., Antochshuk, V. & Jaroniec, M. Block-Copolymer-Templated Ordered Mesoporous Silica: Array of Uniform Mesopores or Mesopore–Micropore Network? *The Journal of Physical Chemistry B* **104**, 11465-11471, doi:10.1021/jp002597a (2000).

45 ChemAxon. *Chemicalize*, <http://www.chemicalize.org/structure/#!mol=CCO%5BSi%5D%28CCCN%29%28OCC%29OCC&source=fp> (2012).

46 Qin, Z. *et al.* Influences of thermal pretreatment temperature and solvent on the organosilane modification of Al13-intercalated/Al-pillared montmorillonite. *Applied Clay Science* **50**, 546-553 (2010).